Prog. Theor. Exp. Phys. **2016**, 043B02 (17 pages)
DOI: 10.1093/ptep/ptw023

Gauge coupling unification in gauge–Higgs grand unification

Naoki Yamatsu*

Department of Physics, Osaka University, Toyonaka, Osaka 560-0043, Japan
*E-mail: yamatsu@het.phys.sci.osaka-u.ac.jp

Received December 21, 2015; Accepted February 16, 2016; Published April 1, 2016

We discuss renormalization group equations for gauge coupling constants in gauge–Higgs grand unification on five-dimensional Randall–Sundrum warped space. We show that all four-dimensional Standard Model gauge coupling constants are asymptotically free and are effectively unified in $SO(11)$ gauge–Higgs grand unified theories on 5D Randall–Sundrum warped space.

Subject Index B40, B42, B43

1. Introduction

Symmetry and its breaking are essential notions in particle physics regardless of theoretical frameworks. The Standard Model (SM) is based on the gauge symmetry $G_{SM} := SU(3)_C \times SU(2)_L \times U(1)_Y$ in four-dimensional (4D) spacetime with the spontaneous electroweak (EW) symmetry breaking G_{SM} to $SU(3)_C \times U(1)_{em}$ via the nonvanishing vacuum expectation value (VEV) of the SM Higgs boson. To construct a unified theory beyond the SM here, we use two notions: gauge–Higgs unification [1–5] and grand unification [6–18]. Gauge–Higgs unification is based on gauge symmetry in higher-dimensional spacetime. For example, the $SU(3)_C \times SO(5)_W \times U(1)_X$ gauge–Higgs electroweak (EW) unified theories on five-dimensional (5D) Randall–Sundrum (RS) warped spacetime are discussed in Refs. [19–25]; the $SU(2)_L \times U(1)_Y$ EW gauge bosons and the SM Higgs boson are unified in 5D $SO(5)_W \times U(1)_X$ bulk gauge bosons, where the RS warped space is introduced in Ref. [26]. Grand unification theory (GUT) is based on grand unified gauge symmetry. The candidates for GUT gauge groups in 4D GUTs are well known (see, e.g., Refs. [6,7]). Also, the candidates for GUT gauge groups in 5D GUTs are shown in Ref. [7]. Gauge–Higgs grand unification [27–34] is based on GUT gauge symmetry in higher-dimensional spacetime. The candidates for GUT gauge groups in 5D gauge–Higgs GUT are shown in Ref. [7]. One of the candidates is an $SO(11)$ group.

An $SO(11)$ gauge-H-iggs grand unified theory (GHGUT) on 5D RS spacetime is proposed by Y. Hosotani and the author in Ref. [34]. In the $SO(11)$ GHGUT, the SM gauge bosons and the SM Higgs boson are unified in the 5D $SO(11)$ bulk gauge boson. The SM Weyl fermions, quarks, and leptons, are unified in an $SO(11)$ bulk fermion for each generation. Proton decay is forbidden by fermion number conservation even if the Kaluza–Klein (KK) scale is much smaller than $O(10^{15})$ GeV.

In this paper, we discuss gauge coupling unification for the 4D SM gauge coupling constants of the zero modes of bulk gauge fields in the gauge–Higgs grand unification scenario, in particular

Funded by SCOAP[3]

$SO(11)$ GHGUTs, by using the renormalization group equations (RGEs) for the 4D gauge coupling constants under KK expansion. We assume that the 4D description is valid up to the fifth-dimensional compactification scale $1/L$ in the 5D RS warped space. The compactification scale $1/L$ is regarded as the real gauge coupling unified scale M_{GUT} because the $SO(11)$ GUT gauge symmetry is broken to the G_{PS} gauge symmetry by the orbifold boundary conditions (BCs) on the Planck and TeV branes, where $G_{PS} := SU(4)_C \times SU(2)_L \times SU(2)_R$ is known as the Pati–Salam gauge group discussed in Ref. [35]. Under the above assumption, we show that in several $SO(11)$ GHGUTs, the SM gauge couplings are asymptotically free at least at one-loop level and the three SM gauge coupling constants take almost the same values below the GUT scale $M_{GUT} = 1/L$ as long as $M_{GUT} = 1/L$ is much larger than its KK mass scale $m_{KK} = \pi k/\left(e^{kL} - 1\right) \simeq \pi k e^{-kL}$, where k is the anti-de Sitter (AdS) curvature in 5D RS warped space.

This paper is organized as follows. In Sect. 2, we discuss an RGE for a gauge coupling constant in 5D non-Abelian gauge theory. In Sect. 3, we discuss RGEs for the SM gauge coupling constants in the $SO(11)$ GHGUT [34], as well as slightly modified ones. We find that the three SM gauge coupling constants are asymptotically free, and they are unified in Sect. 3.1. Their several corrections are studied in Sect. 3.2. Section 4 is devoted to a summary and discussion.

2. RGEs for 4D gauge couplings on 5D RS warped space

Let us first consider a non-Abelian gauge theory on 5D Randall–Sundrum warped spacetime.

We consider a model that contains bulk gauge and fermion fields. Its action is given by

$$\begin{aligned} S &= \int d^5x \sqrt{-\det G}\, \mathcal{L}_{5D} \\ &= \int d^5x \sqrt{-\det G} \left(-\frac{1}{4} \mathrm{Tr} F_{MN} F^{MN} + \overline{\Psi^{(a)}} \mathcal{D}\left(c^{(a)}\right) \Psi^{(a)} + \mathcal{L}_{g.f.} + \mathcal{L}_{gh} \right), \end{aligned} \tag{2.1}$$

where $\mathcal{L}_{g.f.}$ and $\mathcal{L}_{gh}$ stand for gauge-fixing and ghost terms, respectively.

$$\mathcal{D}_M \Psi^{(a)}(x,y) = (\partial_M - igA_M(x,y))\, \Psi^{(a)}(x,y), \tag{2.2}$$

$$A_M(x,y) = \frac{1}{\sqrt{2}} \sum_A A_M^A(x,y) T^A, \tag{2.3}$$

$$F_{MN}(x,y) = \frac{i}{g}\left[\mathcal{D}_M, \mathcal{D}_N\right] = \partial_M A_N - \partial_N A_M - ig\left[A_M, A_N\right] = \frac{1}{\sqrt{2}} \sum_A F_{MN}{}^A(x,y) T^A, \tag{2.4}$$

where $M = 1, 2, \ldots, 5$, T^A are the generators of the Lie group G, its superscript A is the number of generators of G, ξ is the gauge-fixing parameter, and g is the gauge coupling constant.

By using appropriate gauge-fixing and ghost terms discussed in, e.g., Ref. [36], we get the KK mode expansion of the gauge field

$$A_\mu^A(x,z) = \sqrt{\frac{2}{\pi R}} \sum_{n=0}^{\infty} A_\mu^{A(n)}(x) f_n^A(z), \tag{2.5}$$

$$A_z^A(x,z) = \sqrt{\frac{2}{\pi R}} \sum_{n=0}^{\infty} A_\mu^{A(n)}(x) h_n^A(z) \tag{2.6}$$

in a conformal coordinate $z := e^{ky}$ for $|y| \leq L$, where k is the AdS curvature, L is the size of the fifth dimension, and $f_n^A(z)$ and $h_n^A(z)$ are described using Bessel functions (see, e.g., Refs. [23,24]).

Here we summarize some basic results for the RGEs for 4D gauge coupling constants (see, e.g., [6]). We only consider the RGEs at the one-loop level, but we can find the RGEs at the two-loop level given in, e.g., Refs. [37–39]. The RGE for the gauge coupling constant is given by

$$\mu \frac{dg}{d\mu} = \beta(g), \tag{2.7}$$

where $\beta(g)$ is a β function for the gauge coupling constant. In general, a model contains real vector, Weyl fermion, and real scalar fields. The β function at one-loop level is given by

$$\beta^{1-\text{loop}}(g) = -\frac{g^3}{16\pi^2}\left[\frac{11}{3}\sum_{\text{Vector}} T(R_V) - \frac{2}{3}\sum_{\text{Weyl}} T(R_F) - \frac{1}{6}\sum_{\text{Real}} T(R_S)\right], \tag{2.8}$$

where Vector, Weyl, and Real stand for real vector, Weyl fermion, and real scalar fields in terms of 4D theories, respectively. The vector bosons are gauge bosons, so they belong to the adjoint representation of the Lie group G:$T(R_V) = C_2(G)$. $C_2(G)$ is the quadratic Casimir invariant of the adjoint representation of G, and $T(R_i)$ is a Dynkin index of the irreducible representation R_i of G. Note that when the Lie group G is spontaneously broken into its Lie subgroup G', it is convenient to use the irreducible representations of G'. (For its branching rules, see Refs. [7,40].) It is convenient to use the β-function coefficient $b := \left(16\pi^2/g^3\right)\beta^{1-\text{loop}}(g)$ instead of $\beta^{1-\text{loop}}(g)$:

$$b = -\frac{11}{3}\sum_{\text{Vector}} T(R_V) + \frac{2}{3}\sum_{\text{Weyl}} T(R_F) + \frac{1}{6}\sum_{\text{Real}} T(R_S). \tag{2.9}$$

By using $\alpha(\mu) := g^2(\mu)/4\pi$, we can rewrite the RGE in Eq. (2.7) as

$$\frac{d}{d\log(\mu)}\alpha^{-1}(\mu) = -\frac{b}{2\pi}. \tag{2.10}$$

When b is a constant, we can solve it as

$$\alpha^{-1}(\mu) = \alpha^{-1}(\mu_0) - \frac{b}{2\pi}\log\left(\frac{\mu}{\mu_0}\right). \tag{2.11}$$

Let us consider the RGE for the 4D gauge coupling constant in 5D gauge theories given in Eq. (2.10) by using the β function coefficient given in Eq. (2.9), where it depends on its matter content at an energy scale μ. We take into account the contribution to the β function coefficient from not only zero modes but also KK modes for masses less than renormalization scale μ, where since the contribution to the gauge coupling constant of the zero mode from each KK mode is almost the same as that from the zero mode, we neglect the difference between them. Under the approximation, once we know the mass spectra in the models, we can calculate the RGE for the gauge coupling constant at one-loop level. In general, it is difficult to write down exact mass spectra because it depends on orbifold boundary conditions and parameters of bulk and brane terms. For the zeroth approximation, the mass of the zero modes is $m = 0$ and of the kth KK modes is $m = km_{KK}$. By using the mass spectra, the RGE of the gauge coupling constant can be divided into two regions:

$$\frac{d}{d\log(\mu)}\alpha^{-1} \simeq \begin{cases} -\frac{1}{2\pi}b^0 & \text{for} \quad \mu < m_{KK} \\ -\frac{1}{2\pi}\left(b^0 + k\Delta b^{KK}\right) & \text{for} \quad km_{KK} \leq \mu < (k+1)m_{KK} \end{cases}, \tag{2.12}$$

where b^0 is a β-function coefficient given from its zero modes, which can be calculated by using Eq. (2.9); Δb^{KK} is an additional β-function coefficient generated by a set of KK modes of all bulk

Table 1. Summary of the adjoint representation of any Lie group G, where $d(G)$ and $C_2(G)$ stand for the dimension and the quadratic Casimir invariant of the adjoint representation of G. See Refs. [6,7] for details.

Algebra	Group	Rank	$d(G)$	$C_2(G)$
A_n	$SU(n+1)$	$n \geq 1$	$n(n+1)$	$n+1$
B_n	$SO(2n+1)$	$n \geq 3$	$n(2n+1)$	$2n-1$
C_n	$USp(2n)$	$n \geq 2$	$n(2n+1)$	$n+1$
D_n	$SO(2n)$	$n \geq 4$	$n(2n-1)$	$2(n-1)$
E_6	E_6	6	78	12
E_7	E_7	7	133	18
E_8	E_8	8	248	30
F_4	F_4	4	52	9
G_2	G_2	2	14	4

fields, which can also be calculated by using Eq. (2.9). The β-function coefficient Δb^{KK} is

$$\Delta b^{KK} = -\frac{7}{2}C_2(G) + \frac{4}{3}\sum_{\text{Dirac}} T(R) \tag{2.13}$$

because a 5D bulk gauge field is decomposed into 4D gauge and scalar fields and a 5D bulk fermion field is decomposed into 4D Dirac fermion fields.

We solve the RGE in Eq. (2.12). The number of the set of KK modes for $\mu > m_{KK}$ is approximately equal to the energy scale divided by the KK mass scale:

$$k \simeq \frac{\mu}{m_{KK}}. \tag{2.14}$$

We integrate the RGE in Eq. (2.12) with respect to μ from M_Z to μ $\left(M_Z < \mu < m_{KK}\right)$:

$$\alpha^{-1}(\mu) = \alpha^{-1}(M_Z) - \frac{b^0}{2\pi}\log\left(\frac{\mu}{M_Z}\right). \tag{2.15}$$

For $\mu > m_{KK}$, the gauge coupling constant is given by

$$\alpha^{-1}(\mu) \simeq \alpha^{-1}(m_{KK}) - \frac{b^0}{2\pi}\log\left(\frac{\mu}{m_{KK}}\right) - \frac{\Delta b^{KK}}{2\pi}\left(\frac{\mu}{m_{KK}} - 1\right). \tag{2.16}$$

From Eq. (2.16), we find that for $\Delta b^{KK} > 0$, the gauge coupling constant diverges at a certain point,

$$\alpha(\mu) \longrightarrow \infty, \tag{2.17}$$

while for $\Delta b^{KK} < 0$ and $\mu \gg m_{KK}$, the gauge coupling constant reduces rapidly:

$$\alpha(\mu) \simeq \frac{-2\pi}{\Delta b^{KK}}\frac{m_{KK}}{\mu}. \tag{2.18}$$

From Eq. (2.13) and the above discussion, we also find that the gauge coupling constant of a non-Abelian gauge field based on a simple Lie group G is asymptotically free when its matter content satisfies

$$\sum_{\text{Dirac}} T(R) < \frac{21}{8}C_2(G), \tag{2.19}$$

because of $\Delta b^{KK} < 0$. We can check which matter content can satisfy the condition in Eq. (2.19) for any classical and exceptional Lie group by using the quadratic Casimir invariant in Table 1 and the (second-order) Dynkin index of irreducible representations of each simple Lie group G listed in

Ref. [7]. In particular, by using the tables in Appendix A of Ref. [7], it is easy to check the cases for up to rank-15 simple Lie groups and $D_{16} = SO(32)$. Also, by using rank-n discussion, we can check it for any rank classical Lie group.

3. Gauge–Higgs grand unification

Let us consider the RGEs for gauge coupling constants in the $SO(11)$ GHGUT shown in Table 2 and the slightly modified ones by using the results in the previous section. For the energy scale between $M_Z < \mu < m_{KK}$, the RGEs for the SM gauge coupling constants at one-loop level are the same as the RGEs in the SM.

To analyze this difference between the three SM gauge coupling constants, we introduce the following values:

$$\Delta_{ij}(\mu) := \alpha_i(\mu) - \alpha_j(\mu), \tag{3.1}$$

$$\Delta'_{ij}(\mu) := \alpha_i^{-1}(\mu) - \alpha_j^{-1}(\mu), \tag{3.2}$$

where $i, j = 3C, 2L, 1Y$ for the SM gauge coupling constants, $\alpha_i(\mu) = g_i^2/4\pi (i = 3C, 2L, 1Y)$, $\alpha_{3C}(\mu)$ is the $SU(3)_C$ gauge coupling constant, $\alpha_{2L}(\mu)$ is the $SU(2)_L$ gauge coupling constant, $\alpha_{1Y}(\mu)$ is the $U(1)_Y$ gauge coupling constant, and we take the $SU(5)$ normalization for $U(1)_Y$ ($i, j = 4C, 2L, 2R$ for the Pati–Salam gauge coupling constants). From Eqs. (3.1) and (3.2), we have the following relation:

$$\Delta_{ij}(\mu) = -\Delta'_{ij}(\mu)\alpha_i(\mu)\alpha_j(\mu). \tag{3.3}$$

To discuss the accuracy of unification, we introduce $\Xi_{ij}(\mu)$ defined by

$$\Xi_{ij}(\mu) := \frac{\Delta_{ij}(\mu)}{\alpha_j(\mu)} = \frac{\alpha_i(\mu)}{\alpha_j(\mu)} - 1. \tag{3.4}$$

We check the β function coefficients of the three SM gauge coupling constants by using the RGE in Eq. (2.9). The SM matter content or the zero mode matter content in the $SO(11)$ GHGUTs is given in Table 3. By using the formula in Eq. (2.9) and the (second-order) Dynkin indices listed in Refs. [6,7,40], we obtain the following well-known SM β-function coefficients:

$$b_i = -\frac{11}{3}C_2(G_i) + \frac{2}{3}\sum_{\text{Quarks \& Leptons}} T(R_i) + \frac{1}{3}\sum_{\text{Higgs}} T(R_i) = \begin{pmatrix} -7 \\ -19/6 \\ +41/10 \end{pmatrix}, \tag{3.5}$$

where $i = 3C, 2L, 1Y$ stand for $SU(3)_C$, $SU(2)_L$, and $U(1)_Y$, respectively, and we took the $SU(5)$ normalization for $U(1)_Y$.

The RGE evolution for the SM gauge coupling constants in the SM is shown in Fig. 1, where we used the following input parameters for the three SM gauge coupling constants at $\mu = M_Z = 91.1876 \pm 0.0021$ given in Ref. [41]:

$$\alpha_{3C}(M_Z) = 0.1184 \pm 0.0007, \tag{3.6}$$

$$\alpha_{2L}(M_Z) = \frac{\alpha_{em}(M_Z)}{\sin^2\theta_W(M_Z)}, \tag{3.7}$$

$$\alpha_{1Y}(M_Z) = \frac{5\alpha_{em}(M_Z)}{3\cos^2\theta_W(M_Z)}, \tag{3.8}$$

Table 2. The matter content in the $SO(11)$ GHGUT in Ref. [34]. The table on the left shows the matter content of $SO(11)$ bulk fields. Orbifold BC stands for the choice of signs for fermion fields. The table on the right shows the matter content on the Planck brane. (See Ref. [34] for details.)

Bulk field	A_M	$\Psi_{\mathbf{32}}^{(a)}$	$\Psi_{\mathbf{11}}^{(b)}$
$SO(11)$	**55**	**32**	**11**
5D RS	**5**	**4**	**4**
Orbifold BC		$(-,-)$	$(-,-)$
Brane field	$\phi_{\mathbf{16}}$		
$SO(10)$	**16**		
$SL(2,\mathbb{C})$	$(0,0)$		

Table 3. The matter content in the SM or the zero mode matter content in the $SO(11)$ GHGUTs.

	G_μ	W_μ	B_μ	q	u^c	d^c	ℓ	e^c	ϕ
$SU(3)_C$	**8**	**1**	**1**	**3**	$\overline{\mathbf{3}}$	$\overline{\mathbf{3}}$	**1**	**1**	**1**
$SU(2)_L$	**1**	**3**	**1**	**2**	**1**	**1**	**2**	**1**	**2**
$U(1)_Y$	0	0	0	$+1/6$	$-2/3$	$+1/3$	$-1/2$	$+1$	$+1/2$
$SL(2,\mathbb{C})$	$(\frac{1}{2},\frac{1}{2})$	$(\frac{1}{2},\frac{1}{2})$	$(\frac{1}{2},\frac{1}{2})$	$(\frac{1}{2},0)$	$(\frac{1}{2},0)$	$(\frac{1}{2},0)$	$(\frac{1}{2},0)$	$(\frac{1}{2},0)$	$(0,0)$

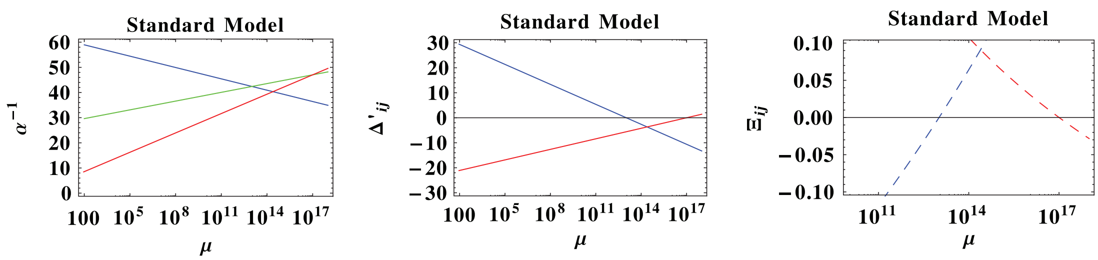

Fig. 1. $\mu-\alpha^{-1}(\mu)$, $\mu-\Delta'_{ij}(\mu)$, $\mu-\Xi_{ij}(\mu)$ (log-linear plots) in the SM. The left figure shows $\mu-\alpha^{-1}(\mu)$ (log-linear plots), where the red line is α_{3C}, the green line is α_{2L}, and the blue line is α_{1Y}; the center figure shows $\mu-\Delta'_{ij}(\mu)$ (log-linear plots), where the red line is $\Delta'_{3C,2L}=\alpha_{3C}^{-1}-\alpha_{2L}^{-1}$ and the blue line is $\Delta'_{1Y,2L}=\alpha_{1Y}^{-1}-\alpha_{2L}^{-1}$; the right figure shows $\mu-\Xi_{ij}(\mu)$ (log-linear plots), where the red line is $\Xi_{3C,2L}=\alpha_{3C}/\alpha_{2L}-1$ and the blue line is $\Xi_{1Y,2L}=\alpha_{1Y}/\alpha_{2L}-1$.

where the relations between the EW gauge coupling constants $\alpha_{2L}(\mu)$ and $\alpha_{1Y}(\mu)$ and the electromagnetic (EM) gauge coupling constant $\alpha_{em}(\mu)$ and the Weinberg angle $\theta_W(\mu)$ are given by

$$\alpha_{em}(\mu)=\frac{3\alpha_{1Y}(\mu)\alpha_{2L}(\mu)}{3\alpha_{1Y}(\mu)+5\alpha_{2L}(\mu)}, \tag{3.9}$$

$$\sin^2\theta_W(\mu)=\frac{3\alpha_{1Y}(\mu)}{3\alpha_{1Y}(\mu)+5\alpha_{2L}(\mu)}. \tag{3.10}$$

The experimental values of the EM gauge coupling constant and the Weinberg angle given in Ref. [41] are

$$\alpha_{em}^{-1}(M_Z)=127.916\pm 0.015, \tag{3.11}$$

$$\sin^2\theta_W(M_Z)=0.23116\pm 0.00013. \tag{3.12}$$

As is well known, GUTs based on the $SU(5)$ gauge group and also other higher-rank gauge groups without intermediate scales predict the SM gauge coupling unification at the GUT scale M_{GUT}. The

Table 4. Summary of representations of the Lie group $SO(11)$ satisfying the condition $T(R) < (21/8)C_2(SO(11) = \mathbf{55}) = 189/8$, where $SO(11)$ Irrep., $d(G)$, $T(R)$, and Type stand for the Dynkin label, the dimension, the Dynkin index, and the type of the irreducible representations of $SO(11)$, respectively. R and PR represent real and pseudo-real representations of $SO(11)$. (See Ref. [7] for details.)

$SO(11)$ Irrep.	$d(G)$	$T(R)$	Type
(10000)	**11**	1	R
(00001)	**32**	4	PR
(01000)	**55**	9	R
(20000)	**65**	13	R

relations between the SM gauge coupling constants $\alpha_i(\mu)$ are given by

$$\alpha_{3C}(M_{GUT}) = \alpha_{2L}(M_{GUT}) = \alpha_{1Y}(M_{GUT}). \tag{3.13}$$

They lead to

$$\sin^2\theta_W(M_{GUT}) = \frac{3}{8}. \tag{3.14}$$

Obviously, $\sin^2\theta_W(M_{GUT}) \neq \sin^2\theta_W(M_Z)$, so we have to take into account the effects for the RGEs for the SM gauge coupling constants between the EW scale and the GUT scale.

At present, the value of $\alpha_i(M_Z)$ has roughly four-digit accuracy, according to Ref. [41]. Thus, it is meaningless to discuss more than four-digit accuracy for $\Xi_{ij}(\mu)$. We regard $^\forall|\Xi_{ij}(\mu)| < 10^{-4}$ as an almost SM gauge coupling unification scale M_{GCU}. From Fig. 1, in the SM, for any scale μ, $^\forall|\Xi_{ij}(\mu)|$ cannot be less than 10^{-4}, and then in the SM without any correction (or only negligible ones), three gauge coupling constants are not unified. If there are intermediate symmetry breaking scales between an original GUT scale and the EW scale, then in general they contribute a non-negligible effect for gauge coupling unification; this is discussed in, e.g., 4D $SO(10)$ GUTs [42–46] because one of the examples is $G_{GUT} = SO(10) \supset G_{PS} \supset G_{SM}$. The rank of the original GUT gauge group G_{GUT} must be more than 4 because the rank of the SM gauge group G_{SM} is 4. The rank of the $SO(11)$ gauge group is 5, so we will discuss its intermediate scale effect in the $SO(11)$ GHGUTs.

3.1. *Asymptotic freedom and gauge coupling unification*

We check the asymptotic freedom condition given in Eq. (2.19) in $SO(11)$ GHGUTs. To maintain the success of the $SO(11)$ gauge–Higgs grand unification in Ref. [34], such as automatic chiral anomaly cancellation for the gauge symmetries on the Planck and TeV branes, we use the same orbifold boundary conditions (BC): the orbifold BC on the Planck brane $y = 0$ breaks $SO(11)$ to $SO(10)$; the orbifold BC on the TeV brane $y = L$ breaks $SO(11)$ to $SO(4) \times SO(7) \simeq SU(2) \times SU(2) \times SO(7)$. The two orbifold BCs break $SO(11)$ to the Pati–Salam gauge group G_{PS}. The orbifold boundary conditions for the $SO(11)$ vector representation **11** on the Planck and TeV branes are given by

$$P_{0\mathbf{11}} = \mathrm{diag}\Big(I_{10}, -I_1\Big), \quad P_{1\mathbf{11}} = \mathrm{diag}\Big(I_4, -I_7\Big). \tag{3.15}$$

Also, by using the branching rules of the representations in Table 4 shown in Ref. [7], we find that the branching rules of pseudo-real representations of $SO(11)$ lead to complex representations of its subgroup, while the branching rules of real representations of $SO(11)$ lead to real representations of its subgroup. That is, we must use pseudo-real representations to realize a 4D chiral gauge theory. In Table 4, only the $SO(11)$ spinor representation **32** is a pseudo-real representation of $SO(11)$. (The $SO(11)$ **320** representation is the second lowest dimensional pseudo-real representation listed

Table 5. Matter contents that satisfy three chiral generations of quarks and leptons and the asymptotic freedom condition in Eq. (3.16).

n_{55}	n_{32}	n_{11}	Δb^{KK}
0	3	0	$-\frac{31}{2}$
0	3	≤ 11	$\frac{-93+8n_{11}}{6}$
0	5	≤ 3	$\frac{-29+8n_{11}}{6}$
1	3	≤ 2	$\frac{-21+8n_{11}}{6}$

Table 6. Matter contents that satisfy three chiral generations of quarks and leptons, the asymptotic freedom condition in Eq. (3.16), and the fermion number conservation.

n_{32}	n_{11}	Δb^{KK}
3	0	$-\frac{31}{2}$
5	≤ 2	$\frac{-13}{6}$
3	≤ 10	$\frac{-93+8n_{10}}{6}$

in Ref. [7].) Also, the zero modes of each $SO(11)$ spinor bulk fermion field are the five SM fermions plus one right-hand neutrino. Therefore, the matter content of $SO(11)$ GHGUTs must contain at least three $SO(11)$ spinor bulk fermion fields, the same as in Ref. [34], so we subtract the contribution from the three $SO(11)$ spinor bulk fermion fields. The asymptotic freedom condition is

$$\sum_R T(R) < \frac{93}{8}. \tag{3.16}$$

We consider which matter contents can satisfy the asymptotic freedom condition in Eq. (3.16). To maintain the number of chiral matter fields, if we introduce an $SO(11)$ spinor bulk fermion field with a parity assignment, then we must also introduce another $SO(11)$ spinor bulk fermion field with the opposite parity assignment. From Table 4, the $SO(11)$ **65** representation does not satisfy the condition. By using the condition in Eq. (3.16) and the Dynkin indices given in Table 2, we summarize the matter contents in Table 5 that satisfy three chiral generations of quarks and leptons and the asymptotic freedom condition in Eq. (3.16).

In the $SO(11)$ GHGUT [34], fermion number conservation leads to sufficient proton decay suppression [34]. When we impose the fermion number conservation, an $SO(11)$ **55** bulk fermion with orbifold BCs must have another $SO(11)$ **55** bulk fermion with the opposite orbifold BCs; an $SO(11)$ **11** bulk fermion with orbifold BCs must have another $SO(11)$ **11** bulk fermion with the opposite orbifold BCs. From Table 5, we cannot introduce any $SO(11)$ **55** bulk fermion to keep the fermion number conservation without exotic fermion zero modes. The matter contents that satisfy three chiral generations of quarks and leptons, the asymptotic freedom condition in Eq. (3.16), and the fermion number conservation are shown in Table 6.

As in the previous section, we use approximate mass spectra of zero modes and kth KK modes whose masses are $m = 0$ and $m = km_{KK}$, respectively. We also use the gauge coupling constant in

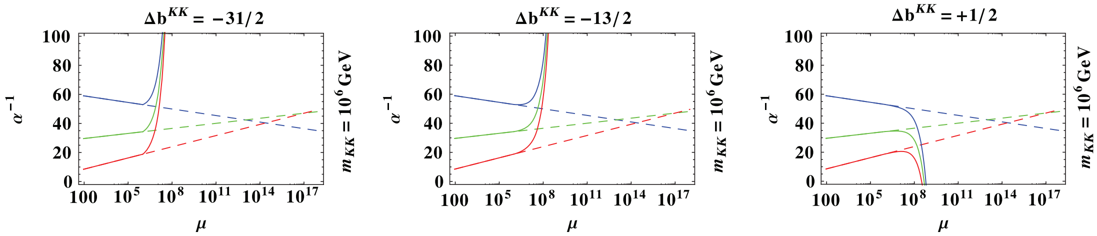

Fig. 2. $\mu - \alpha^{-1}(\mu)$ (log-linear plots) in $SO(11)$ GHGUTs with one KK mass scale $m_{kk} = 10^{10}$ GeV: the left, center, and right figures show $(n_{32}, n_{11}) = (3, 0)$ $\left(\Delta b^{KK} = -31/2\right)$, $(n_{32}, n_{11}) = (5, 2)$ $\left(\Delta b^{KK} = -13/6\right)$, and $(n_{32}, n_{11}) = (5, 4)$ $\left(\Delta b^{KK} = +1/2\right)$, respectively, where the solid lines show the $SO(11)$ GHGUTs; the dashed lines show the SM ones; the red lines stand for α_{3C}; the green lines stand for α_{2L}; and the blue lines stand for α_{1Y}.

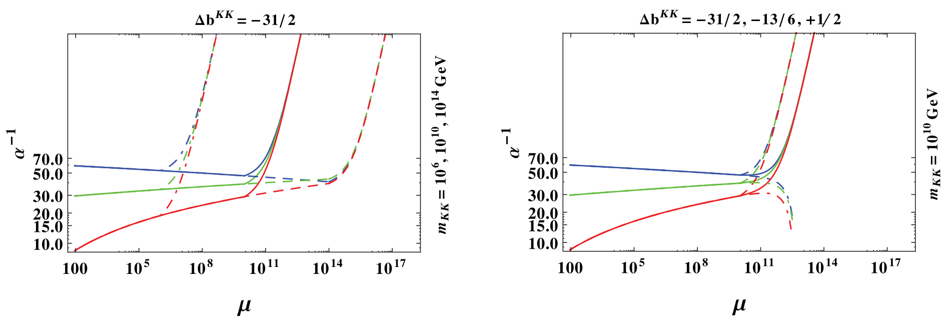

Fig. 3. $\mu - \alpha^{-1}(\mu)$ (log-log plots) in $SO(11)$ GHGUTs: the right figure shows three different matter contents $(n_{32}, n_{11}) = (3, 0)$ $\left(\Delta b^{KK} = -31/2\right)$, $(n_{32}, n_{11}) = (5, 2)$ $\left(\Delta b^{KK} = -13/6\right)$, and $(n_{32}, n_{11}) = (5, 4)$ $\left(\Delta b^{KK} = +1/2\right)$, with a fixed KK mass $m_{KK} = 10^{10}$ GeV, where the dashed lines show $\Delta b^{KK} = -31/2$, the solid lines show $\Delta b^{KK} = -13/6$, and the dash-dotted lines show $\Delta b^{KK} = +1/2$; the left figure shows one matter content $(n_{32}, n_{11}) = (3, 0)$ $\left(\Delta b^{KK} = -31/2\right)$, with three different KK masses $m_u = 10^6, 10^{10}, 10^{14}$ GeV, where the dashed lines show $m_{KK} = 10^6$ GeV, the solid lines show $m_{KK} = 10^{10}$ GeV, and the dash-dotted lines show $m_{KK} = 10^{14}$ GeV. For both figures, the red lines stand for α_{3C}; the green lines stand for α_{2L}; and the blue lines stand for α_{1Y}.

Eq. (2.16) for the three SM gauge group, where α^{-1}, b^0, and Δb^{KK} should be replaced by α_i^{-1}, b_i^0, and Δb^{KK}. α_i^{-1} and b_i^0 are dependent on the SM gauge group, while Δb^{KK} is independent of the SM gauge group. From Eq. (2.16), we find that the difference between the $SO(11)$ GHGUTs and the SM is only in its third term dependent on Δb^{KK} for $\mu > m_{KK}$. Also, the difference between α_i^{-1} and α_j^{-1} $(i \neq j)$ in the $SO(11)$ GHGUTs is in the first and second terms in Eq. (2.16). Therefore, $\Delta'_{ij}(\mu)$ in the $SO(11)$ GHGUTs are the same as those in the SM. ($\Delta'_{ij}(\mu)$ in the SM are shown in the center figure in Fig. 1.) By using the asymptotic form of the gauge coupling constant given in Eq. (2.18), for $\mu \gg m_{KK}$, $\Xi_{ij}(\mu)$ can be written as

$$\Xi_{ij}(\mu) \simeq -\Delta'_{ij}(\mu)\left(\frac{-2\pi}{\Delta b^{SO(11)}}\frac{m_{KK}}{\mu}\right). \tag{3.17}$$

Let us check what we can learn from Figs. 2, 3, and 4. From Fig. 2, we can clearly see that the three SM gauge coupling constants $\alpha_i (i = 3C, 2L, 1Y)$ are convergent into one, and rapidly decreasing for $\Delta b^{KK} < 0$ and increasing for $\Delta b^{KK} > 0$, as shown in Eqs. (2.18) and (2.17), respectively. From the

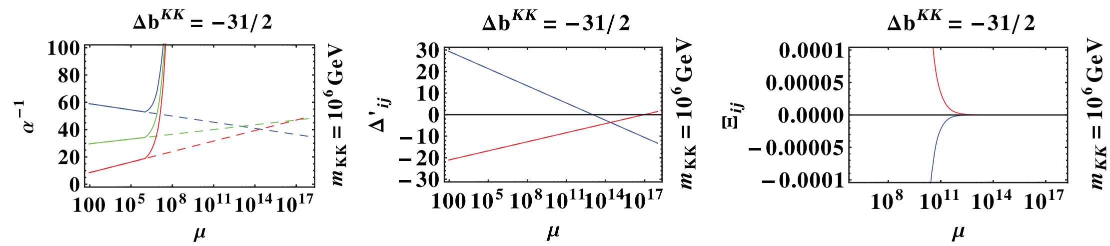

Fig. 4. $\mu-\alpha^{-1}(\mu)$, $\mu-\Delta'_{ij}(\mu)$, and $\mu-\Xi_{ij}(\mu)$ (log-linear plots) in $SO(11)$ GHGUT with the same matter content $\left(n_{\mathbf{32}}, n_{\mathbf{11}}\right)=(3,0)$ $\left(\Delta b^{KK}=-31/2\right)$ and KK mass $m_{KK}=10^6$ GeV: the left figure shows $\mu-\alpha^{-1}(\mu)$ (log-linear plots), where the red line represents α_{3C}, the green line represents α_{2L}, and the blue line represents α_{1Y}; the center figure shows $\mu-\Delta'_{ij}(\mu)$ (log-linear plots), where the red line is $\Delta'_{3C,2L}=\alpha_{3C}^{-1}-\alpha_{2L}^{-1}$ and the blue line is $\Delta'_{1Y,2L}=\alpha_{1Y}^{-1}-\alpha_{2L}^{-1}$; the right figure shows $\mu-\Xi_{ij}(\mu)$ (log-linear plots), where the red line is $\Xi_{3C,2L}=\alpha_{3C}/\alpha_{2L}-1$ and the blue line is $\Xi_{1Y,2L}=\alpha_{1Y}/\alpha_{2L}-1$. The dashed lines show the SM, the solid lines show $SO(11)$ GHGUT.

left figure in Fig. 3, we find that for $\Delta b^{KK}<0$, the SM gauge coupling constants decrease drastically above m_{KK} and they also converge, where the convergent scales depend on Δb^{KK}; for $\Delta b^{KK}>0$, the SM gauge coupling constants increase drastically and also seem to converge above m_{KK}, where our perturbative calculation is not reliable. From the right figure in Fig. 3, we find that, regardless of KK mass scales $m_{KK}=10^6, 10^{10}, 10^{14}$ GeV, the SM gauge coupling constants decrease drastically above m_{KK} and they also converge for $\Delta b^{KK}<0$, where they diverge for $\Delta b^{KK}>0$. From the right figure in Fig. 4, we find that for $\mu\sim 10^{10.5}$ GeV, $\Xi_{ij}(\mu)\sim 10^{-4}$, so we regard $\mu>10^{10.5}$ GeV as M_{GCU} in this case. The center figure in Fig. 4 is exactly the same as that in Fig. 1. One may wonder that even in the $SO(11)$ GHGUTs, the gauge coupling constants were not unified based on Fig. 4. For the $SO(11)$ GHGUTs, from the definition of $\Delta'_{ij}(\mu)$ in Eq. (3.2) and the four-digit accuracy of $\alpha_i(M_Z)$, the error of $\Delta'_{ij}(\mu)$ is $\mathrm{Err}[\Delta'_{ij}(\mu)]\simeq O\left(10^{-4}\right)\alpha^{-1}(\mu)\simeq O\left(10^{-4}\right)\mu/m_{KK}$ for $\mu>M_{GCU}\gg m_{KK}$. For $m_{KK}=10^6$ GeV and $\mu=10^{11}$ GeV, $\mathrm{Err}\left[\Delta'_{ij}\left(10^{11}\text{ GeV}\right)\right]\simeq O(10)$ and the deviations $\Delta'_{3C,2L}\left(10^{11}\text{ GeV}\right)$ and $\Delta'_{1Y,2L}\left(10^{11}\text{ GeV}\right)$ are less than 10 from the center figure in Fig. 4, and then M_{GCU} starts around 10^{11} GeV.

From the above discussion, we found that in the $SO(11)$ GHGUTs the 4D SM gauge coupling constants are almost unified above M_{GCU} regardless of the matter contents and their mass spectra, and the SM gauge coupling constants are asymptotically free. We also found that M_{GCU} depends on the matter contents given in Table 5.

3.2. *Corrections for gauge coupling constants*

We check whether the above analysis is valid even when we take into account several corrections. We divide our discussion into two cases, $m_{KK}<M_{PS}\simeq M_{GUT}=1/L$ and $m_{KK}<M_{PS}<M_{GUT}=1/L$, where M_{PS} is the symmetry breaking scale at which G_{PS} gauge symmetry is broken in G_{SM} gauge symmetry. This is because for $m_{KK}<M_{GUT}=1/L\simeq M_{PS}$, we use only the RGEs for the G_{SM} gauge coupling constants, while for $m_{KK}<M_{PS}<M_{GUT}=1/L$, we have to use the RGEs for the G_{SM} gauge coupling constants below M_{PS} and the RGEs for the G_{PS} gauge coupling constants above M_{PS}. In the latter analysis, we have to take into account matching the conditions between the G_{PS} gauge coupling constraints and the G_{SM} gauge coupling constraints at the Pati–Salam scale M_{PS}. (Note that for 4D non-SUSY $SO(10)$ GUTs, this effect has been discussed in many articles, e.g., Refs. [42–48].)

3.2.1. $m_{KK} < M_{GUT} \simeq M_{PS} \simeq 1/L$

Here we check whether the above analysis is valid even when we take into account mass spectra of bulk fields. Since mass spectra in the $SO(11)$ GHGUTs depend on orbifold BCs and parameters of bulk and brane terms, it is almost impossible to use them in an exact expression. Instead, we use approximate forms for the flat space limit. We use the mass spectra of the kth KK modes ($k = 1, 2, \ldots$) of bulk fields by their orbifold BCs for the flat space limit:

$$(N, D), (D, N) : \frac{2k-1}{2} m_{KK}, \tag{3.18}$$

$$(N, N), (D, D) : k m_{KK}, \tag{3.19}$$

where N and D stand for Neumann and Dirichlet BCs, respectively. (X, Y) $(X, Y = N, D)$ stands for the orbifold BCs on the Planck and TeV branes, respectively. (This approximation is good for large k because the RS warped space is an asymptotically flat space for a short distance.) Only each field with (N, N) contains a zero mode. For large k, a kth KK mass spectrum in RS warped space approaches that in flat space. For most cases, the difference between warped and flat spaces leads to only a tiny effect for RGEs because the contribution to the β-function coefficient from each mode is logarithmic. In the following discussion, we use the above approximate mass spectra.

By using the above approximation for the mass spectra of the bulk fields, the RGE for the gauge coupling constant can be divided into three regions:

$$\frac{d}{d\log(\mu)}\alpha_i^{-1} \simeq \begin{cases} -\dfrac{1}{2\pi} b_i^0 & \text{for} \quad \mu < \dfrac{m_{KK}}{2} \\ -\dfrac{1}{2\pi}\left(b_i^0 + \delta b_i^{\rm KK} + (k-1)\,\Delta b^{\rm KK}\right) & \text{for} \quad \left(k - \dfrac{1}{2}\right) m_{KK} \le \mu < k m_{KK}, \\ -\dfrac{1}{2\pi}\left(b_i^0 + k\Delta b^{\rm KK}\right) & \text{for} \quad k m_{KK} \le \mu < \left(k + \dfrac{1}{2}\right) \end{cases} \tag{3.20}$$

where b_i^0 is the β-function coefficients given from its zero modes, i.e., bulk fields with the orbifold BC (N, N); $\delta b_i^{\rm KK}$ is the β-function coefficient by bulk fields with the orbifold BC (N, D) or (D, N); $\Delta b^{\rm KK}$ is the additional β-function coefficient generated by a set of KK modes of all bulk fields, where b_i^0, $\delta b_i^{\rm KK}$, and $\Delta b^{\rm KK}$ can be calculated by using Eq. (2.9).

We solve the RGE in Eq. (3.20). As in Sect. 2, the number of the set of KK modes for $\mu > m_{KK}$ is approximately equal to the energy scale divided by the KK mass scale $k \simeq \mu/m_{KK}$ in Eq. (2.14). Under the approximation, we can solve the RGE exactly, but that seems to make it difficult to see the contribution from mass splitting effects. We only write down a rough approximate form for $m_{KK} \ge \mu$,

$$\alpha_i^{-1}(\mu) \simeq \alpha_i^{-1}(m_{KK}) - \left(\frac{b_i^0}{2\pi} + \frac{\delta b_i^{KK}}{4\pi}\right)\log\left(\frac{\mu}{m_{KK}}\right) - \frac{\Delta b^{\rm KK}}{2\pi}\left(\frac{\mu}{m_{KK}} - 1\right), \tag{3.21}$$

where, for $M_Z < \mu < m_{KK}$,

$$\alpha_i^{-1}(\mu) = \alpha_i^{-1}(M_Z) - \frac{1}{2\pi} b_i^0 \log\left(\frac{\mu}{M_Z}\right). \tag{3.22}$$

(For the above expression, we ignored the contribution to $\alpha_i(\mu)$ from δb_i^{KK} between $m_{KK}/2$ and m_{KK}, and so on.) We find that the first and second terms in Eq. (3.21) are negligible compared with the third term for large μ.

Table 7. The orbifold BCs of the components of the $SO(11)$ bulk gauge field $A_M = A_\mu \oplus A_y$.

Field	BC	Representations of $G_{SM} = SU(3)_C \times SU(2)_L \times U(1)_Y$
A_μ	(N, N)	$(\mathbf{8}, \mathbf{1})_0$, $(\mathbf{1}, \mathbf{1})_0$, $(\mathbf{1}, \mathbf{3})_0$
	(N, D)	$(\mathbf{3}, \mathbf{2})_{-5/6}$, $(\bar{\mathbf{3}}, \bar{\mathbf{2}})_{+5/6}$
	(D, N)	$(\mathbf{3}, \mathbf{1})_{-1/3}$, $(\bar{\mathbf{3}}, \bar{\mathbf{1}})_{+1/3}$
	(D_{eff}, N)	$(\mathbf{3}, \mathbf{1})_{+2/3}$, $(\bar{\mathbf{3}}, \bar{\mathbf{1}})_{-2/3}$, $(\mathbf{1}, \mathbf{1})_{+1}$, $(\mathbf{1}, \mathbf{1})_{-1}$, $(\mathbf{1}, \mathbf{1})_0$
	(D, D)	$(\mathbf{1}, \mathbf{2})_{+1/2}$, $(\mathbf{2}, \mathbf{1})_{-1/2}$
	(D_{eff}, D)	$(\mathbf{3}, \mathbf{2})_{+1/6}$, $(\bar{\mathbf{3}}, \bar{\mathbf{2}})_{-1/6}$
A_y	(N, N)	$(\mathbf{1}, \mathbf{2})_{+1/2}$, $(\mathbf{2}, \mathbf{1})_{-1/2}$
	(N, D)	$(\mathbf{3}, \mathbf{1})_{-1/3}$, $(\bar{\mathbf{3}}, \bar{\mathbf{1}})_{+1/3}$
	(D, N)	$(\mathbf{3}, \mathbf{2})_{-5/6}$, $(\bar{\mathbf{3}}, \bar{\mathbf{2}})_{+5/6}$, $(\mathbf{3}, \mathbf{2})_{+1/6}$, $(\bar{\mathbf{3}}, \bar{\mathbf{2}})_{-1/6}$
	(D, D)	$(\mathbf{8}, \mathbf{1})_0$, $(\mathbf{1}, \mathbf{1})_0$, $(\mathbf{1}, \mathbf{3})_0$, $(\mathbf{3}, \mathbf{1})_{+2/3}$, $(\bar{\mathbf{3}}, \bar{\mathbf{1}})_{-2/3}$, $(\mathbf{1}, \mathbf{1})_{+1}$, $(\mathbf{1}, \mathbf{1})_{-1}$, $(\mathbf{1}, \mathbf{1})_0$

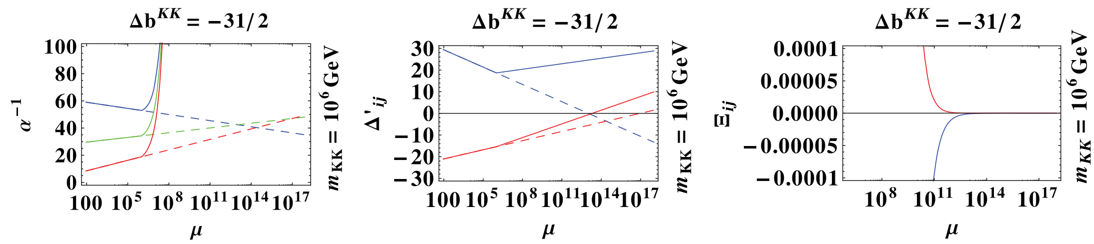

Fig. 5. $\mu - \alpha^{-1}(\mu)$, $\mu - \Delta'_{ij}(\mu)$, $\mu - \Xi_{ij}(\mu)$ (log-linear plots) in the $SO(11)$ GHGUT with the matter content $(n_{32}, n_{11}) = (3, 0)$ $\left(\Delta b^{KK} = -31/2\right)$ and KK mass $m_{KK} = 10^6$ GeV, and bulk gauge field mass splitting correction. For the explanation, see the caption in Fig. 4.

By using the above discussion, we calculate how much the mass splitting effect by the orbifold BCs contributes to the gauge coupling unification. First, we need to know the contribution for δb_i^{KK} from the $SO(11)$ bulk gauge fields and the $SO(11)$ **32** and **11** bulk fermion fields, but as long as the fermion number is preserved and their brane Dirac mass terms change the component fields with a Neumann BC to those with an effective Dirichlet BC on the Planck brane, they lead to the same contribution to all three gauge coupling constants: $\delta b_{1L}^{KK} = \delta b_{2L}^{KK} = \delta b_{3C}^{KK}$. Therefore, we consider the contribution to δb_i^{KK} $(i = 3C, 2L, 1Y)$ from the $SO(11)$ bulk gauge field. From Table 7, we get

$$\delta b_{3C}^{KK} = -\frac{83}{6}, \quad \delta b_{2L}^{KK} = -10, \quad \delta b_{1Y}^{KK} = -\frac{437}{15}. \tag{3.23}$$

From Fig. 5, we find the following. First, from the center figure, $\mu - \Delta'_{ij}(\mu)$, in Fig. 5, we find that the δb_i^{KK} term in Eq. (3.21) is not negligible compared with the b_i^0 term, and contributes to $\Delta'_{ij}(\mu)$. From the right figures, $\mu - \Xi_{ij}(\mu)$, in Figs. 4 and 5, the convergence scale is changed, but this does not affect whether the SM gauge coupling constants converge or not. Therefore, we find that orbifold BCs or mass spectra affect the detail structure of gauge couplings described by $\Delta'_{ij}(\mu)$, but they do not affect the convergence of the SM gauge coupling constants described by $\Xi_{ij}(\mu)$.

We comment on the contribution to RGEs from the $SO(10)$ spinor brane scalar field on the Planck brane in Table 2. Its non-vanishing VEV is responsible for breaking $SO(10)$ to $SU(5)$. There are 21 would-be NG modes. Nine modes are eaten by G_{PS}/G_{SM} gauge bosons, while 12 modes are uneaten because $SO(10)/G_{PS}$ gauge bosons absorb their corresponding fifth-dimensional components of the 5D gauge field. The 12 modes become massive via their quantum correction, whose

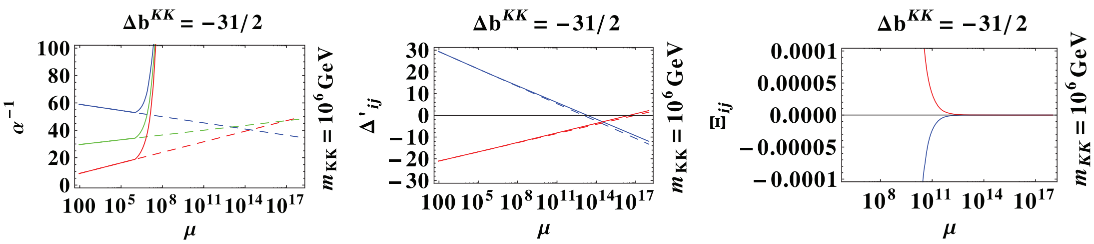

Fig. 6. $\mu - \alpha^{-1}(\mu)$, $\mu - \Delta'_{ij}(\mu)$, $\mu - \Xi_{ij}(\mu)$ (log-linear plots) in the $SO(11)$ GHGUT with the matter content $\left(n_{32}, n_{11}\right) = (3, 0)$ $\left(\Delta b^{KK} = -31/2\right)$ and KK mass $m_{KK} = 10^6$ GeV, and would-be NG correction. For the explanation, see the caption in Fig. 4.

Table 8. The SM matter content in the Pati–Salam base.

	G'_μ	W_μ	W'_μ	q'	$u^{c\prime}$	ϕ'
$SU(4)_C$	**15**	**1**	**1**	**4**	$\overline{\mathbf{4}}$	**1**
$SU(2)_L$	**1**	**3**	**1**	**2**	**1**	**2**
$SU(2)_R$	**1**	**1**	**3**	**1**	**2**	**2**
$SL(2,\mathbb{C})$	$\left(\frac{1}{2},\frac{1}{2}\right)$	$\left(\frac{1}{2},\frac{1}{2}\right)$	$\left(\frac{1}{2},\frac{1}{2}\right)$	$\left(\frac{1}{2},0\right)$	$\left(\frac{1}{2},0\right)$	$(0,0)$

masses are expected to be $O(m_{KK})$ or less depending on the dynamics. They correspond to a complex scalar field with $(\mathbf{3},\mathbf{2})_{-1/6}$ under G_{SM}. It is not any $SU(5)$ multiplet, and it affects the gauge coupling unification. The contribution to the β-function coefficients of G_{SM} is given by

$$b_i^{\text{wNG}} = \frac{1}{3}\sum_{\text{would-be NG}} T(R_i) = \begin{pmatrix} +1/3 \\ +1/2 \\ +1/5 \end{pmatrix}, \tag{3.24}$$

where this contribution effectively vanishes above the brane mass scale of $\phi_{\mathbf{16}}$ because the $SO(10)$ full multiplet **16** contributes to the β-function coefficients of G_{SM}. From Fig. 6, we find that it contributes to a gauge coupling unification scale, but the values of b_i^{wNG} are small.

3.2.2. $m_{KK} < M_{PS} < M_{GUT} \simeq 1/L$

Let us discuss the Pati–Salam scale M_{PS} effect. In this case, we have to use different RGEs for the SM and Pati–Salam gauge coupling constants above and below M_{PS}.

We check the β-function coefficients of the Pati–Salam gauge coupling constants of the zero modes by using the RGE in Eq. (2.9). The matter content of the zero mode is shown in Table 8. By using the formula in Eq. (2.9) and the Dynkin indices listed in Refs. [6,7,40], we obtain

$$b_i = -\frac{11}{3}C_2(G_i) + \frac{2}{3}\sum_{\text{Weyl Fermions}} T(R_i) + \frac{1}{3}\sum_{\text{Complex Scalar}} T(R_i) = \begin{pmatrix} -32/3 \\ -19/6 \\ -19/6 \end{pmatrix}, \tag{3.25}$$

where $i = 4C, 2L, 2R$ stand for $SU(4)_C$, $SU(2)_L$, and $SU(2)_R$, respectively.

We consider the contribution to δb_i^{KK} from the mass spectra of the $SO(11)$ bulk gauge field. As we discussed before, the would-be NG bosons do not affect the RGEs for the SM gauge coupling constants. We can calculate δb_i^{KK} $(i = 4C, 2L, 2R)$ by using the orbifold BCs of the $SO(11)$ bulk gauge

Table 9. The orbifold BCs of the components of the $SO(11)$ bulk gauge field $A_M = A_\mu \oplus A_y$ in the Pati–Salam base.

Field	BC	Representations of G_{PS}
A_μ	(N, N)	$(\mathbf{15}, \mathbf{1}, \mathbf{1})$, $(\mathbf{1}, \mathbf{3}, \mathbf{1})$, $(\mathbf{1}, \mathbf{1}, \mathbf{3})$
	(N, D)	$(\mathbf{6}, \mathbf{2}, \mathbf{2})$
	(D, N)	$(\mathbf{6}, \mathbf{1}, \mathbf{1})$
	(D, D)	$(\mathbf{1}, \mathbf{2}, \mathbf{1})$
A_y	(N, N)	$(\mathbf{1}, \mathbf{2}, \mathbf{2})$
	(N, D)	$(\mathbf{6}, \mathbf{1}, \mathbf{1})$
	(D, N)	$(\mathbf{6}, \mathbf{2}, \mathbf{2})$
	(D, D)	$(\mathbf{15}, \mathbf{1}, \mathbf{1})$, $(\mathbf{1}, \mathbf{3}, \mathbf{1})$, $(\mathbf{1}, \mathbf{1}, \mathbf{3})$

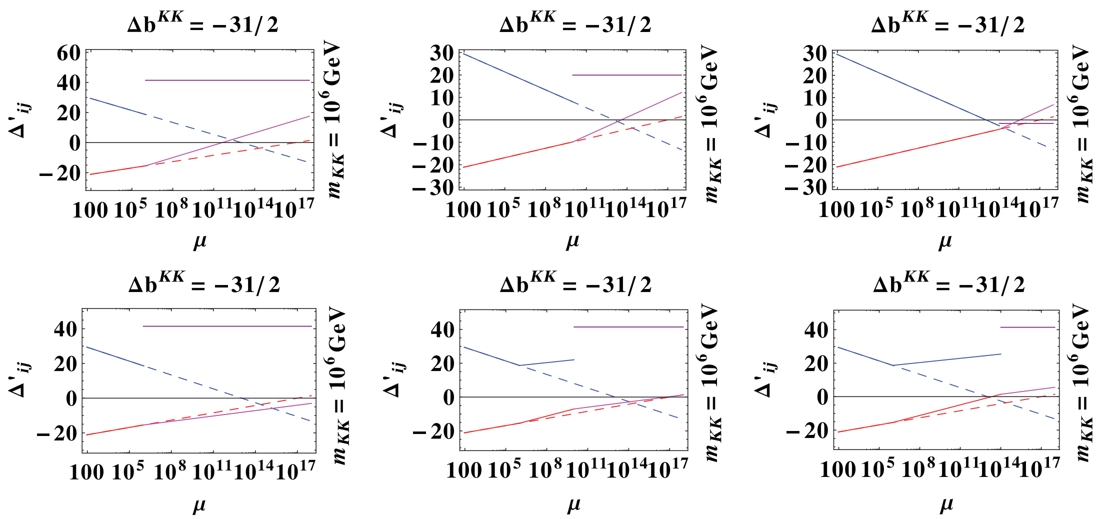

Fig. 7. $\mu - \Delta'_{ij}(\mu)$ (log-linear plots) in $SO(11)$ GHGUT with the same matter content $\left(n_{32}, n_{11}\right) = (3, 0)$ $\left(\Delta b^{KK} = -31/2\right)$ and KK mass $m_{KK} = 10^6$ GeV, and Pati–Salam scales $M_{PS} = 10^6, 10^{10}, 10^{14}$ GeV: the top figures do not include the $SO(11)$ bulk gauge field mass splitting correction; the bottom figures include the $SO(11)$ bulk gauge field mass splitting correction. The red line is $\Delta'_{3C,2L} = \alpha_{3C}^{-1} - \alpha_{2L}^{-1}$, the blue line is $\Delta'_{1Y,2L} = \alpha_{1Y}^{-1} - \alpha_{2L}^{-1}$, the purple line is $\Delta'_{2R,2L} = \alpha_{2R}^{-1} - \alpha_{2L}^{-1}$, and the magenta line is $\Delta'_{4C,2L} = \alpha_{4C}^{-1} - \alpha_{2L}^{-1}$.

field shown in Table 9:

$$\delta b_{4C}^{KK} = -\frac{35}{3}, \quad \delta b_{2L}^{KK} = -21, \quad \delta b_{2R}^{KK} = -21. \tag{3.26}$$

We have to use the RGEs for three SM gauge coupling constants below M_{PS}, while we have to use the RGEs for three Pati–Salam gauge coupling constants. To connect them, we use the following matching condition at the Pati–Salam scale M_{PS} ($m_{KK} < M_{PS} < M_{GUT}$):

$$\alpha_{3C}(M_{PS}) = \alpha_{4C}(M_{PS}), \tag{3.27}$$

$$\alpha_{2L}(M_{PS}) = \alpha'_{2L}(M_{PS}), \tag{3.28}$$

$$\alpha_{1Y}^{-1}(M_{PS}) = \frac{3}{5}\alpha_{2R}^{-1}(M_{PS}) + \frac{2}{5}\alpha_{4C}^{-1}(M_{PS}), \tag{3.29}$$

where they are determined by the normalization conditions of the generators of G_{PS} and G_{SM} (see, e.g., Ref. [44] for details).

From the $\mu - \Delta'_{ij}(\mu)$ figures in Fig. 7, we find that the Pati–Salam scale without the orbifold BCs (mass splitting) affect the detail structure of gauge couplings described by $\Delta'_{ij}(\mu)$. Thus, even when we take into account the Pati–Salam scale, the orbifold BCs, etc., they do not change our discussion about asymptotic freedom of the SM gauge coupling constants and gauge coupling unification. For $m_{KK} = 10^6$ GeV and $\mu = 10^{11-12}$, $\text{Err}\left[\Delta'_{ij}\left(10^{11-12}\,\text{GeV}\right)\right] \simeq O(10\text{–}100)$ and the deviations $\Delta'_{3C,2L}\left(10^{11-12}\,\text{GeV}\right)$ and $\Delta'_{1Y,2L}\left(10^{11-12}\,\text{GeV}\right)$ are less than 50 from the center figure in Fig. 7, and then M_{GCU} starts around 10^{11-12} GeV.

4. Summary and discussion

We discussed the RGEs for the 4D SM gauge coupling constants in the $SO(11)$ gauge–Higgs grand unification scenario on the 5D RS warped spacetime. We found that the 4D SM gauge coupling constants are asymptotically free in the $SO(11)$ GHGUTs with the matter contents shown in Tables 5 and 6, which satisfy $\Delta b^{KK} < 0$. We also discussed the SM gauge coupling unification. We showed that the three SM gauge coupling constants are effectively unified above the almost SM gauge coupling unification scale M_{GCU} discussed in Sect. 3.1. We have not fixed the GUT or compactification scale $M_{GUT} = 1/L$, but as long as $M_{GUT} = 1/L$ is larger than M_{GCU}, there is no inconsistency within at least the current experimental accuracy of the SM gauge coupling constants. In Sect. 3.2, we showed that the correction from the mass spectra of the $SO(11)$ bulk gauge fields, the would-be NG boson, and the Pati–Salam scale does not affect the asymptotic freedom and gauge coupling unification of the SM gauge couplings, while they affect the detail structures of the RGE running. From the above, we find that the Weinberg angle at $\mu = M_{GUT}$, $\sin^2\theta_W(M_{GUT}) = 3/8$, is consistent with that at $\mu = M_Z$, $\sin^2\theta_W(M_Z) \simeq 0.23$.

In this paper, we mainly considered the $SO(11)$ GHGUTs, but our discussion can be applied to other GHGUTs. For example, we have already found the asymptotic freedom condition for a gauge coupling constant in general GHGUTs based on any simple Lie group G in Eq. (2.19). It is very easy to list the the matter contents that satisfy the asymptotic freedom condition by using the tables in Ref. [7].

We discussed the RGEs for the 4D SM gauge coupling constants in 5D RS warped spacetime by using the KK expansion. There is another approach using AdS/CFT-like correspondence, as discussed in Refs. [49–53].

Acknowledgements

The author would like to thank Yutaka Hosotani for many stimulating discussions and valuable comments, and also thanks Hidenori Fukaya, Taichiro Kugo, Minoru Tanaka, and Satoshi Yamaguchi for useful comments. This work was supported in part by Japan Society for the Promotion of Science Grant-in-Aid for Scientific Research No. 23104009.

Funding

Open Access funding: SCOAP[3].

References

[1] Y. Hosotani, Phys. Lett. B **126**, 309 (1983).
[2] Y. Hosotani, Ann. Phys. **190**, 233 (1989).
[3] A. T. Davies and A. McLachlan, Phys. Lett. B **200**, 305 (1988).
[4] A. T. Davies and A. McLachlan, Nucl. Phys. B **317**, 237 (1989).
[5] H. Hatanaka, T. Inami, and C. S. Lim, Mod. Phys. Lett. A **13**, 2601 (1998) [arXiv:hep-th/9805067] [Search INSPIRE].
[6] R. Slansky, Phys. Rept. **79**, 1 (1981).

[7] N. Yamatsu, [arXiv:1511.08771 [hep-ph]] [Search INSPIRE].
[8] H. Georgi and S. L. Glashow, Phys. Rev. Lett. **32**, 438 (1974).
[9] K. Inoue, A. Kakuto, and Y. Nakano, Prog. Theor. Phys. **58**, 630 (1977).
[10] H. Fritzsch and P. Minkowski, Ann. Phys. **93**, 193 (1975).
[11] M. Ida, Y. Kayama, and T. Kitazoe, Prog. Theor. Phys. **64**, 1745 (1980).
[12] Y. Fujimoto, Phys. Rev. D **26**, 3183 (1982).
[13] F. Gursey, P. Ramond, and P. Sikivie, Phys. Lett. B **60**, 177 (1976).
[14] N. Maekawa and T. Yamashita, Prog. Theor. Phys. **107**, 1201 (2002) [arXiv:hep-ph/0202050] [Search INSPIRE].
[15] Y. Kawamura, Prog. Theor. Phys. **103**, 613 (2000) [arXiv:hep-ph/9902423] [Search INSPIRE].
[16] Y. Kawamura, Prog. Theor. Phys. **105**, 999 (2001) [arXiv:hep-ph/0012125] [Search INSPIRE].
[17] Y. Kawamura, Prog. Theor. Phys. **105**, 691 (2001) [arXiv:hep-ph/0012352] [Search INSPIRE].
[18] N. Yamatsu, Prog. Theor. Exp. Phys. **2013**, 123B01 (2013) [arXiv:1304.5215 [hep-ph]] [Search INSPIRE].
[19] K. Agashe, R. Contino, and A. Pomarol, Nucl. Phys. B **719**, 165 (2005) [arXiv:hep-ph/0412089] [Search INSPIRE].
[20] Y. Hosotani, K. Oda, T. Ohnuma, and Y. Sakamura, Phys. Rev. D **78**, 096002 (2008) [arXiv:0806.0480 [hep-ph]] [Search INSPIRE].
[21] S. Funatsu, H. Hatanaka, Y. Hosotani, Y. Orikasa, and T. Shimotani, Phys. Lett. B **722**, 94 (2013) [arXiv:1301.1744 [hep-ph]] [Search INSPIRE].
[22] Y. Matsumoto and Y. Sakamura, J. High Energy Phys. **08**, 175 (2014) [arXiv:1407.0133 [hep-ph]] [Search INSPIRE].
[23] S. Funatsu, H. Hatanaka, Y. Hosotani, Y. Orikasa, and T. Shimotani, Phys. Rev. D **89**, 095019 (2014) [arXiv:1404.2748 [hep-ph]] [Search INSPIRE].
[24] S. Funatsu, H. Hatanaka, Y. Hosotani, Y. Orikasa, and T. Shimotani, Prog. Theor. Exp. Phys. **2014**, 113B01 (2014) [arXiv:1407.3574 [hep-ph]] [Search INSPIRE].
[25] S. Funatsu, H. Hatanaka, and Y. Hosotani, Phys. Rev. D **92**, 115003 (2015) [arXiv:1510.06550 [hep-ph]] [Search INSPIRE].
[26] L. Randall and R. Sundrum, Phys. Rev. Lett. **83**, 3370 (1999) [arXiv:hep-ph/9905221] [Search INSPIRE].
[27] G. Burdman and Y. Nomura, Nucl. Phys. B **656**, 3 (2003) [arXiv:hep-ph/0210257] [Search INSPIRE].
[28] N. Haba, M. Harada, Y. Hosotani, and Y. Kawamura, Nucl. Phys. B **657**, 169 (2003) [arXiv:hep-ph/0212035] [Search INSPIRE].
[29] N. Haba, Y. Hosotani, Y. Kawamura, and T. Yamashita, Phys. Rev. D **70**, 015010 (2004) [arXiv:hep-ph/0401183] [Search INSPIRE].
[30] C. Lim and N. Maru, Phys. Lett. B **653**, 320 (2007) [arXiv:0706.1397 [hep-ph]] [Search INSPIRE].
[31] K. Kojima, K. Takenaga, and T. Yamashita, Phys. Rev. D **84**, 051701 (2011) [arXiv:1103.1234 [hep-ph]] [Search INSPIRE].
[32] M. Frigerio, J. Serra, and A. Varagnolo, J. High Energy Phys. **06**, 029 (2011) [arXiv:1103.2997 [hep-ph]] [Search INSPIRE].
[33] K. Yamamoto, Nucl. Phys. B **883**, 45 (2014) [arXiv:1401.0466 [hep-th]] [Search INSPIRE].
[34] Y. Hosotani and N. Yamatsu, Prog. Theor. Exp. Phys. **2015**, 111B01 (2015) [arXiv:1504.03817 [hep-ph]] [Search INSPIRE].
[35] J. C. Pati and A. Salam, Phys. Rev. D **10**, 275 (1974).
[36] Y. Hosotani, S. Noda, and N. Uekusa, Prog. Theor. Phys. **123**, 757 (2010) [arXiv:0912.1173 [hep-ph]] [Search INSPIRE].
[37] M. E. Machacek and M. T. Vaughn, Nucl. Phys. B **222**, 83 (1983).
[38] M. E. Machacek and M. T. Vaughn, Nucl. Phys. B **236**, 221 (1984).
[39] M. E. Machacek and M. T. Vaughn, Nucl. Phys. B **249**, 70 (1985).
[40] W. G. McKay and J. Patera, *Tables of Dimensions, Indices, and Branching Rules for Representations of Simple Lie Algebras* (Marcel Dekker, Inc., New York, 1981).
[41] K. A. Olive et al. [Particle Data Group Collaboration], Chin. Phys. C **38**, 090001 (2014).
[42] N. Deshpande, E. Keith, and P. B. Pal, Phys. Rev. D **46**, 2261 (1993).
[43] N. Deshpande, E. Keith, and P. B. Pal, Phys. Rev. D **47**, 2892 (1993) [arXiv:hep-ph/9211232] [Search INSPIRE].

[44] R. N. Mohapatra, *Unification and Supersymmetry: The Frontiers of Quark–Lepton Physics* (Springer, New York, 2002).
[45] G. Altarelli and D. Meloni, J. High Energy Phys. **1308**, 021 (2013) [arXiv:1305.1001 [hep-ph]] [Search INSPIRE].
[46] D. Meloni, T. Ohlsson, and S. Riad, J. High Energy Phys. **12**, 052 (2014) [arXiv:1409.3730 [hep-ph]] [Search INSPIRE].
[47] Y. Mambrini, N. Nagata, K. A. Olive, J. Quevillon, and J. Zheng, Phys. Rev. D **91**, 095010 (2015) [arXiv:1502.06929 [hep-ph]] [Search INSPIRE].
[48] K. S. Babu and S. Khan, Phys. Rev. D **92**, 075018 (2015) [arXiv:1507.06712 [hep-ph]] [Search INSPIRE].
[49] L. Randall and M. D. Schwartz, Phys. Rev. Lett. **88**, 081801 (2002) [arXiv:hep-th/0108115] [Search INSPIRE].
[50] L. Randall and M. D. Schwartz, J. High Energy Phys. **0111**, 003 (2001) [arXiv:hep-th/0108114] [Search INSPIRE].
[51] W. D. Goldberger and I. Z. Rothstein, Phys. Rev. Lett. **89**, 131601 (2002) [arXiv:hep-th/0204160] [Search INSPIRE].
[52] W. D. Goldberger and I. Z. Rothstein, Phys. Rev. D **68**, 125011 (2003) [arXiv:hep-th/0208060] [Search INSPIRE].
[53] W. D. Goldberger, Y. Nomura, and D. Tucker-Smith, Phys. Rev. D **67**, 075021 (2003) [arXiv:hep-ph/0209158] [Search INSPIRE].